SEMICLASSICAL DESCRIPTIONS OF ATOMIC AND NUCLEAR COLLISIONS
J. Bang & J. de Boer (editors)

ABSORPTIVE POTENTIALS

Giovanni POLLAROLO

Istituto di Fisica Teorica, Universita' di Torino, Italy, INFN, Sezione di Torino, Italy

Abstract. A model [1,2]) for the absorptive part of the optical potential for heavy-ion scattering will be reviewed. It will be shown how, in these reactions, the absorption is dominated by the excitation of the nuclear surface degrees of freedom like inelastic scattering to collective states and one-nucleon transfer-reactions. It will also be discussed how useful this microscopic model of absorption is in providing a starting point for the selfconsistent description of grazing collisions. As examples the scattering of ^{16}O on several targets and at several bombarding energies will be shown.

1. INTRODUCTION

The optical potential is one of the most useful theoretical tools for the analysis of grazing reactions among heavy ions. It is used to construct the wave functions of relative motion and it is usually inferred by fitting elastic scattering data.

Expanding the wave function of relative motion in partial waves, the elastic angular distribution can be written as:

$$\frac{d\sigma_{el}}{d\Omega} \simeq \left| \frac{i}{2k} \sum_l (2l+1) S_l P_l(cos\theta) \right|^2$$

where $k = \sqrt{2\mu E/\hbar^2}$ is the wave number and θ the scattering angle. The S-matrix element S_l is related to the total phase shift δ_l,

$$S_l = e^{2i\delta_l} \quad . \tag{1}$$

It is convenient to write the total phase shift

$$\delta_l = \delta_l^C + \delta_l^N \tag{2}$$

as a sum of the Coulomb and Nuclear components. In WKB approximation the nuclear phase shift can be directly related to the ion-ion potential. In fact in the approximation of a weak potential we can write [3]),

$$\delta_l^N = -\frac{1}{2\hbar} \int_{-\infty}^{+\infty} U^N(r(t))dt \tag{3}$$

where the time integral has to be performed along the classical trajectory $\vec{r}(t)$.

Since the total reaction cross-section is different from zero, the phase shifts must be complex numbers, the imaginary part describing the loss of flux in the elastic channel due to the other reaction channels. This, in accordance with the above formula, can easily be obtained allowing the potential to be a complex function,

$$U^N_{opt}(r) = U^N(r) + iW(r) . \tag{4}$$

The imaginary part of the phase shift is thus simply given by,

$$Im\delta_l = -\frac{1}{2\hbar}\int_{-\infty}^{+\infty} W(r(t))dt \tag{5}$$

and the probability P_0 for remaining in the elastic channel for the given partial wave l is,

$$P_0 = exp\left\{+\frac{2}{\hbar}\int_{-\infty}^{+\infty} W(r(t))dt\right\} . \tag{6}$$

From the systematic analysis of elastic-scattering data one has learnt that these potentials are quite well described by a local function of r of Woods-Saxon shape. Its parameters cannot, however, be unambiguously determined since the elastic-scattering data are sensitive only to the tail of the potential. Nevertheless one knows that the real part is energy independent and presents a smooth variation from system to system. The imaginary part, reflecting the number of open reaction channels, is instead energy dependent and has large variations from system to system.

The real part of the optical potential has been related succesfully to the ground-state densities of the two interacting nuclei and to the nucleon-nucleon interaction through a double-folding model. Since the imaginary part of the optical potential has to describe the depopulation of the entrance channel, a folding model is inadequate for its description. This has to be done taking into account the structure of the two interacting nuclei and of those that can be reached in a transfer process.

It is possible to distinguish [1]) two major mechanisms contribuiting to the imaginary potential, a volume term W_v due to the mean free path of the nucleons in nuclear matter, and a surface part

$$W_s = W_{inel} + W_{trans} \tag{7}$$

due to the additional contribution of inelastic and transfer channels. The volume component has been studied by solving the Bethe-Goldstone equation for two nuclear matter systems in relative motion[4]) or by using complex energy-functionals [5]). The imaginary potentials so calculated are short ranged since the surface effects, like the excitation of the collective modes, are not included in such calculations. On the other hand one expects that in heavy-ion reactions the absorption is mainly concentrated

on the surface of the two ions because all final channels, including fusion, can hardly be reached except via channels excited during the approach of the nuclear surfaces. Candidates for the associated processes are inelastic excitations of surface vibrations and transfer of individual nucleons. Note that these processes are responsible for the large energy loss encountered in the deep-inelastic reactions.

2. THE MODEL

To illustrate how the reaction channels are related to the absorptive part of the optical potential we will consider the simple case of a low-frequency monopole vibration. This case, although very simple, contains all the steps one has to take in the specification of an equivalent optical potential and the generalisation to actual situations is straightforward.

For a monopole vibration, the surface of the nucleus, e. g. the target A, can be parametrized as,

$$R_A(\alpha) = R_0(1 + \alpha/\sqrt{4\pi}) \tag{8}$$

where R_0 is the equilibrium radius and α the deformation parameter. Since the frequency of the mode is small we can apply the sudden approximation [6]) and consider the scattering in the deformed potential corresponding to a given deformation α. In this case the S-matrix element (1) will be a function of α with the phase shift (3), given by

$$\delta_l(\alpha) = -\frac{1}{2\hbar}\int_{-\infty}^{+\infty} U(\alpha, r(t))dt \tag{9}$$

where the nuclear potential is parametrized as usual,

$$U(\alpha, r) = -U_0 exp\left\{-\frac{r - R_A(\alpha)}{a}\right\} . \tag{10}$$

The elastic S-matrix element is thus

$$S_l^{el} = < 0 \mid S_l(\alpha) \mid 0 > = \int_{-\infty}^{+\infty} f_0(\alpha) S_l(\alpha) d\alpha . \tag{11}$$

Here $f_0(\alpha)$ represents the probability to have a given deformation α in the ground state $\mid 0 >$ of the vibrator,

$$f_0(\alpha) = \frac{1}{< \alpha > \sqrt{2\pi}} exp\left\{-\frac{\alpha^2}{2 < \alpha >^2}\right\}$$

where

$$< \alpha > = \sqrt{\frac{\hbar\omega}{2C}} \tag{12}$$

is the zero-point amplitude of the mode.

The matrix element (11) can be evaluated by expanding the phase shift $\delta_l(\alpha)$ up to second order in α. One obtains,

$$S_l^{el} \simeq exp\left\{2i\left[\delta_l + i\left(<\alpha>\frac{\partial\delta_l}{\partial\alpha}\right)^2\right]\right\} . \tag{13}$$

Thus the coupling of the relative motion to the monopole mode of the target generates a complex elastic phase shift $\overline{\delta}_l$ with the imaginary part

$$Im\overline{\delta}_l = \left(<\alpha>\frac{\partial\delta_l}{\partial\alpha}\right)^2 \tag{14}$$

describing the flux absorbed from the elastic channel in to the inelastic excitation of the monopole mode. From the comparison of this result with (5) we get that the imaginary part of the "equivalent" optical potential has to satisfy the following condition,

$$\int_{-\infty}^{+\infty} W(r(t))dt = -\frac{<\alpha>^2}{2\hbar}\left(\int_{-\infty}^{+\infty}\frac{\partial U(r)}{\partial\alpha}dt\right)^2 . \tag{15}$$

In order to take into account the effect of the finite frequency of the mode it is convenient to solve the above problem in the semiclassical approximation. In this approximation, valid in the limit where the wavelength of relative motion is very small, the interaction responsible for the excitation of the mode is time dependent as the two ions move on the classical trajectory $\vec{r}(t)$. The population of the nuclear state is described by a set of coupled differential equations in time for the amplitude. For harmonic vibrations this set of coupled equations can be solved explicitly to give for the probability to have N phonons

$$P_N = \frac{|a(+\infty)|^{2N}}{N!}e^{-|a(+\infty)|^2} . \tag{16}$$

The amplitude $a(+\infty)$ is

$$a(+\infty) = \frac{<\alpha>}{\hbar}\int_{-\infty}^{+\infty}\frac{\partial U(r)}{\partial\alpha}e^{i\omega t}dt \tag{17}$$

with the potential $U(r)$ given by (10). In particular the probability to remain in the elastic channel is given by

$$P_0 = exp\left\{-\frac{<\alpha>^2}{\hbar^2}\left|\int_{-\infty}^{+\infty}\frac{\partial U(r)}{\partial\alpha}e^{i\omega t}dt\right|^2\right\} . \tag{18}$$

From the comparison of (18) with (6) we get for the imaginary part of the optical potential the condition,

$$\int_{-\infty}^{+\infty} W(r(t))dt = -\frac{<\alpha>^2}{2\hbar}\left|\int_{-\infty}^{+\infty}\frac{\partial U(r)}{\partial\alpha}e^{i\omega t}dt\right|^2 \tag{19}$$

that coincides with (15) in the sudden approximation.

It is from this relation, or equivalently from (15), that we are able to extract an expression for $W(r)$. As it stands, this formula is inadequate to specify $W(r)$. For each l we only know the integral of W. So to be useful this relation has to be supplemented with additional hypotheses. An attractive one is suggested by the empirical observation that most of the elastic-scattering angular-distributions can be described by an l-independent local potential.

This additional constraint is enforced on (15) by observing that, due to the exponential decay of the formfactor, the main contribution to the integral on the right-hand side comes from a small region around the turning point r_0 of the classical trajectory. This fact allows us to use a parabolic approximation for the classical trajectory and write

$$r = r_0 + \frac{1}{2}\ddot{r}_0 t^2 \quad , \tag{20}$$

where $\ddot{r}_0$ is the acceleration at the turning point r_0. With this approximation equation (15) is transformed into an integral equation related to a Weyl transform[7]). This integral equation can be solved approximately[1]) to give

$$W_{inel}(r) \simeq -\sqrt{\frac{\pi a}{\hbar^2 \ddot{r}_0}}\left(\frac{\partial U}{\partial r}\right)^2 \sigma^2 \tag{21}$$

with

$$\sigma^2 = \frac{<\alpha>^2 R_0^2}{4\pi} exp\left\{-\frac{a\omega^2}{\ddot{r}_0}\right\} \tag{22}$$

representing the zero-point fluctuation amplitude in the nuclear radius weighted by the adiabatic cut-off function that takes into account the finite frequency of the mode. The parameter a is the diffuseness of the nuclear potential ($a = 0.6fm$). In (21) the subscript *inel* has been added to remind us that this expression holds only for inelastic channels. With this result we can conclude that the scattering in the field U with the coupling to the monopole mode of the target is equivalent to the potential scattering in the field $U + iW$ with W given by (21).

The generalization of the above result to other vibrational degrees of freedom besides the monopole can be done quite easily in the semiclassical approximation [1]). The final result coincides with (21) but now the fluctuation in the sum of the nuclear radii is given by

$$\sigma^2 = \sum_\lambda \frac{2\lambda+1}{4\pi}\left\{\frac{\hbar\omega_\lambda^a}{2C_\lambda^a}(R_a^0)^2 + \frac{\hbar\omega_\lambda^A}{2C_\lambda^A}(R_A^0)^2\right\} g(\lambda, \hbar\omega_\lambda) \tag{23}$$

where the adiabatic cut-off function g also accounts for the contribution from the different μ components of the modes.

The particle-transfer degrees of freedom are very important in the evolution of the reaction between heavy ions both in the quasi-elastic and deep-inelastic regime. In our description of the absorption [1]) the particle- transfer degrees of freedom can be incorporated substituting in (21) the inelastic formfactor $\sqrt{4\pi}\sigma(\partial U/\partial r)$ with the one-particle transfer formfactor $f_\lambda(r)$,

$$W_{trans} = \sum_{a,a',\lambda} \sqrt{\frac{a_{tr}(a_1, a_1')}{16\pi\hbar^2 \ddot{r}_0}} \left\{ (2j_1' + 1) U(a_1)^2 V(a_1')^2 \mid f_\lambda^{(a_1, a_1')}(r) \mid^2 \right\} g(\lambda, Q) \quad (24)$$

where the summation has to be extended over all one-particle transitions between projectile and target. The single-particle levels connected by the transition are labelled by $a_1 \equiv (n_1, l_1, j_1)$, with n_1 indicating the number of nodes, while l_1 and j_1 are the orbital and total angular momenta. The quantity a_{tr} is the diffuseness of the formfactor ($a_{tr} \simeq 1.2fm$) associated with the reactions connecting the single-particle states a_1 and a_1'. The parameters U^2 and V^2 are the spectroscopic factors. Thus, V^2 gives the probability that a given orbital is occupied and $U^2 = (1 - V^2)$ is the corresponding probability that the orbital is empty. The adiabatic cutoff function $g(\lambda, Q)$ weighs the probability with which the different transfer channels contribute, at a given bombarding energy, to W_{trans}.

The two mechanisms contributing to W in (21) and (24) are both of exponential shape in the tail region. The inelastic contribution is short-ranged with a decay-length $a \simeq 0.3fm$ while the transfer contribution is longer-ranged with $a \simeq 0.6fm$. This implies that in most cases transfer reactions dominate the absorption.

In the discussion of the inelastic component of W we have left out the Coulomb interaction. Due to its long range ($\sim 1/r^{\lambda+1}$), the parabolic approximation used above cannot be applied. Fortunately, at low bombarding energies, the Coulomb interaction can be neglected in most projectile and target combinations. This is not the case for the rotational degrees of freedom. They lead to a much larger probability to remain in the elastic channel than equation (18) would predict[3]). The transition amplitude $a(+\infty)$ displays an oscillatory behaviour as a function of the initial angular momentum and does not lead to a simple parametrization of $W(r)$. The rotational degrees of freedom should therefore be treated explicitly with coupled-channel calculations.

3. APPLICATIONS

We have shown that the imaginary part of the optical potential $W(r)$ is related to the square of the formfactors entering in a DWBA analysis of grazing collisions (inelastic scattering and one-particle transfer reactions). Thus the elastic scattering and the grazing collisions have to be described simultaneously in a selfconsistent way,

and the deformation parameters and the spectroscopic factors used in the calculation of $W(r)$ have to be the ones obtained from the analysis of the data.

3.1. *The* $^{16}O + ^{88}Sr$ *reaction.*

The reaction $^{16}O + ^{88}Sr$ has been studied in great detail. The elastic-scattering angular distribution, the inelastic scattering to the low-lying states of ^{88}Sr, and the one-proton stripping- reactions, have been measured[8,9]) at several bombarding energies.

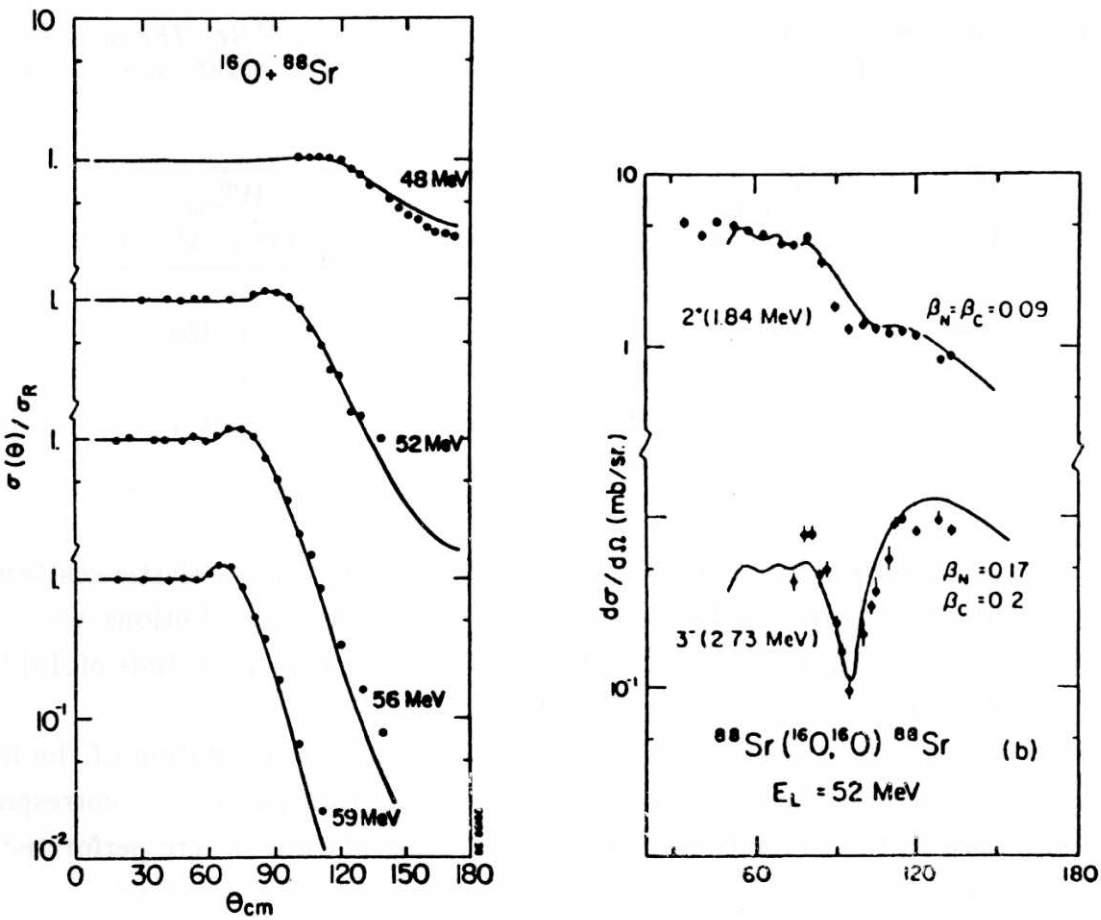

Fig. 1. *A) Ratio of elastic to Rutherford angular distributions for the reaction* $^{16}O + ^{88}Sr$ *at different bombarding energies. The datapoints are from ref.* [8,9]). *B) Differential cross sections for inelastic scattering at a bombarding energy of 52 MeV. The deformation parameters used are indicated. The datapoints are from ref.* [9]).

In order to evaluate the component of the imaginary potential coming from the mass-transfer degrees of freedom we need the one-particle transfer formfactors connecting the different single-particle states in target and projectile. To get these formfactors an experimental set of single-particle energies have been used for the two nuclei. The corresponding single-particle wave-functions were obtained by utilizing a standard Woods-Saxon potential ($r_0 = 1.25fm$, $a = 0.65fm$) with the strength parameter V_0 adjusted to fit the experimental binding energies. Using unity spectroscopic factors the imaginary potentials of Table I have been obtained for the different bombarding energies. The parameters listed in the Table correspond to a Woods-Saxon best fit to our calculated points. For the component coming from the inelastic degrees of freedom the experimental information on the excited states of projectile and target has been used. In the last column of Table I is shown the constant W^0_{inel} that multiplies the square of the inelastic formfactor $\partial U/\partial r$ (cfr. eq. (21)).

Table I. *The absorptive potential for the reaction of* ^{16}O *on* ^{88}Sr. *The parameters corresponding to a Woods-Saxon best fit to our calculated points are given for various bombarding energies.*

E_{Lab} (MeV)	W^0_{trans} (MeV)	r_0 (fm)	a_W (fm)	W^0_{inel} (fm^2MeV^{-1})
48	−21.30	1.23	0.53	−0.026
52	−23.37	1.23	0.53	−0.031
56	−28.80	1.23	0.52	−0.034
59	−34.70	1.23	0.52	−0.036

In Fig. 1a are shown, for the bombarding energies indicated, the elastic-scattering angular-distributions (ratio to Rutherford). These angular distributions were obtained from an optical-model calculation[11]) with the imaginary potentials of Table 1 and with the double-folding real potential of Ref. [10]).

The corresponding angular distributions for the inelastic excitation of the low-lying states in ^{88}Sr are shown in Fig. 1b. The deformation parameters correspond to the ones used in the evaluation of W_{inel}. These calculations where performed in the DWBA with the standard prescription for the inelastic formfactor, i.e.

$$f_{inel}(r) = \frac{\partial U_{opt}}{\partial r} = \frac{\partial U}{\partial r} + i\frac{\partial W}{\partial r}$$

The use of an imaginary formfactor is consistent with our description of the absorption, in fact it can be shown[12]) that this part of the off-diagonal coupling-interaction is related to a two-step transfer from the target to the projectile and back to the target.

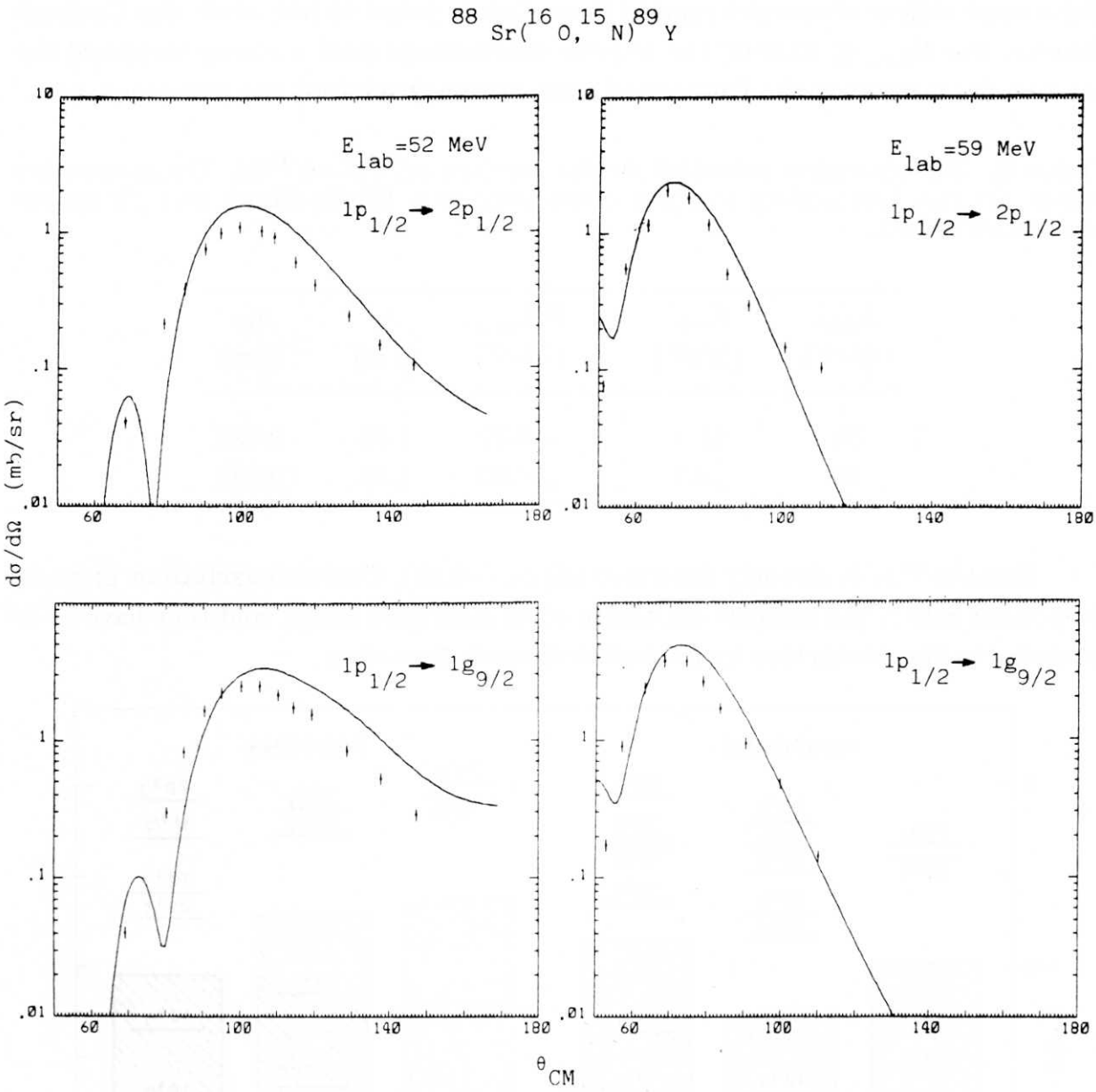

Fig. 2. *Differential cross sections for one-proton stripping in the reaction of* $^{16}O + ^{88}Sr$ *at two bombarding energies and for two single-particle transitions. The curves correspond to full-recoil calculations. The spectroscopic factors have been assumed to be unity. The datapoints are from ref.* [8]).

For two of the bombarding energies indicated in Fig. 1a the one-proton stripping reaction to the ground state and to the first excited state of ^{89}Y have been calculated[13]). These full-recoil calculations were performed utilyzing the code ONEFF and DWIRI[13]). The angular distributions obtained are shown in Fig. 2 along with the datapoints. In agreement with the calculation of W_{trans} the spectroscopic factors have been assumed to be unity.

3.2. *The* $^{16}O + ^{28}Si$ *reaction.*

Complete angular distributions for the reaction $^{16}O + ^{28}Si$ have been obtained[15])

for a large variety of energies ranging from slightly below to well above the Coulomb barrier. For $E_{c.m.} \leq 35 MeV$ the angular distributions show a strong backward rise up to a few percent of the Rutherford cross section (backward rise phenomenon).

Table II. *The absorptive potential for the reaction of* ^{16}O *on* ^{28}Si. *The parameters given for two bombarding energies correspond to a Woods-Saxon best fit to our calculated points.*

E_{Lab} (MeV)	$E_{c.m.}$ (MeV)	W^0_{trans} (MeV)	r_0 (fm)	a_W (fm)
33	21.1	−0.50	1.08	0.550
36	22.7	−1.60	1.08	0.525

Because ^{28}Si is strongly deformed ($\beta_2 \simeq -0.35$), Coulomb excitation plays an important role in the inelastic excitation of its rotational states, and they have to be included in the description by a coupled-channels formalism.

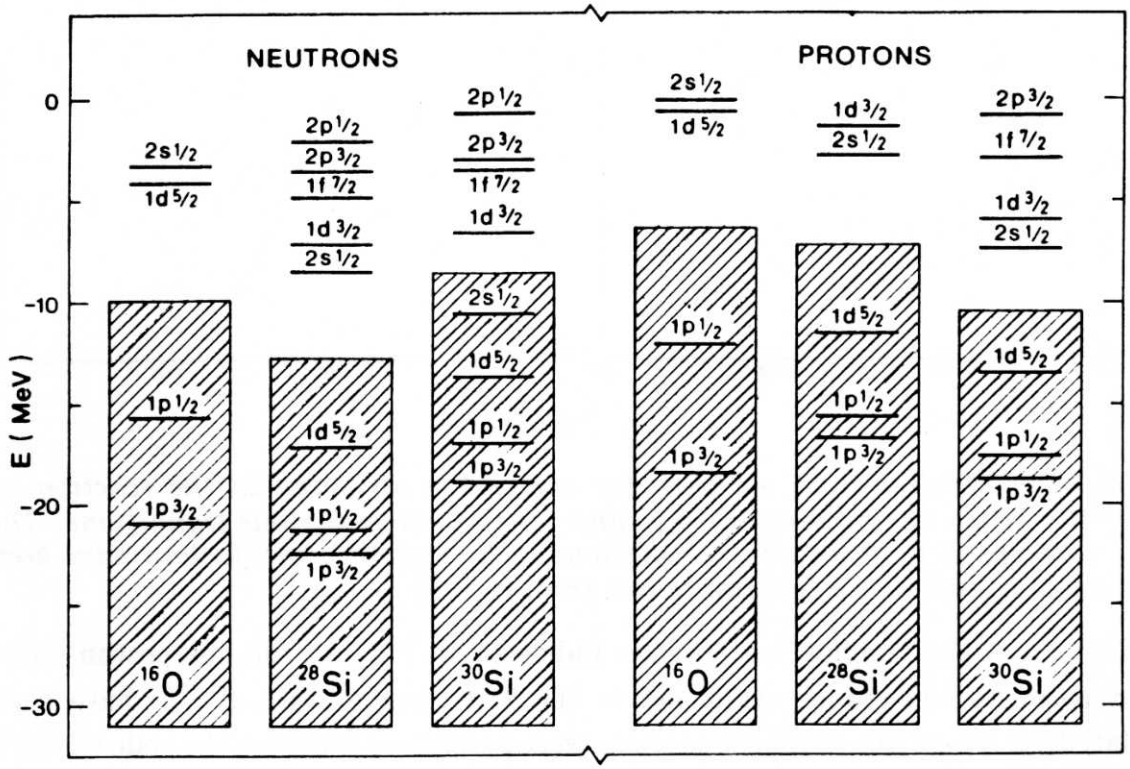

Fig. 3. *Experimental single-particle levels for neutrons and protons in* ^{16}O *and* $^{28,30}Si$, *used in the calculation of the absorptive potential.*

In these calculations only W_{trans} is needed since the other degrees of freedom are taken into account explicitly . In Fig. 3 are shown the "experimental" energies of the single-particle orbitals of ^{16}O and ^{28}Si entering in the calculation of W_{trans}.

To obtain the single-particle wave functions needed to construct the formfactors, a spherical Woods-Saxon potential with parameters $r_0 = 1.25fm$ and $a = 0.65fm$ was used. The depth was adjusted to fit the binding energies. Unity spectroscopic factors were used. The obtained parameters for the Woods-Saxon best fit to our calculated points are summarized in Table II.

The calculations[16]) of the angular distributions were carried out in a coupled-channels formalism using for the real part of the optical potential the one of ref. [10]) in its Woods-Saxon parametrization and for the imaginary part the one of Table II. For the Coulomb component the standard prescription has been used with a small Coulomb radius ($r_{0C} = 0.8fm$). Both the real and the imaginary potentials were deformed according to the shape of ^{28}Si ($\beta_2 = -0.38$). The $2^+, 4^+$ and the 6^+ members of the rotational band of ^{28}Si were included in the calculation with all the corresponding reorientation terms.

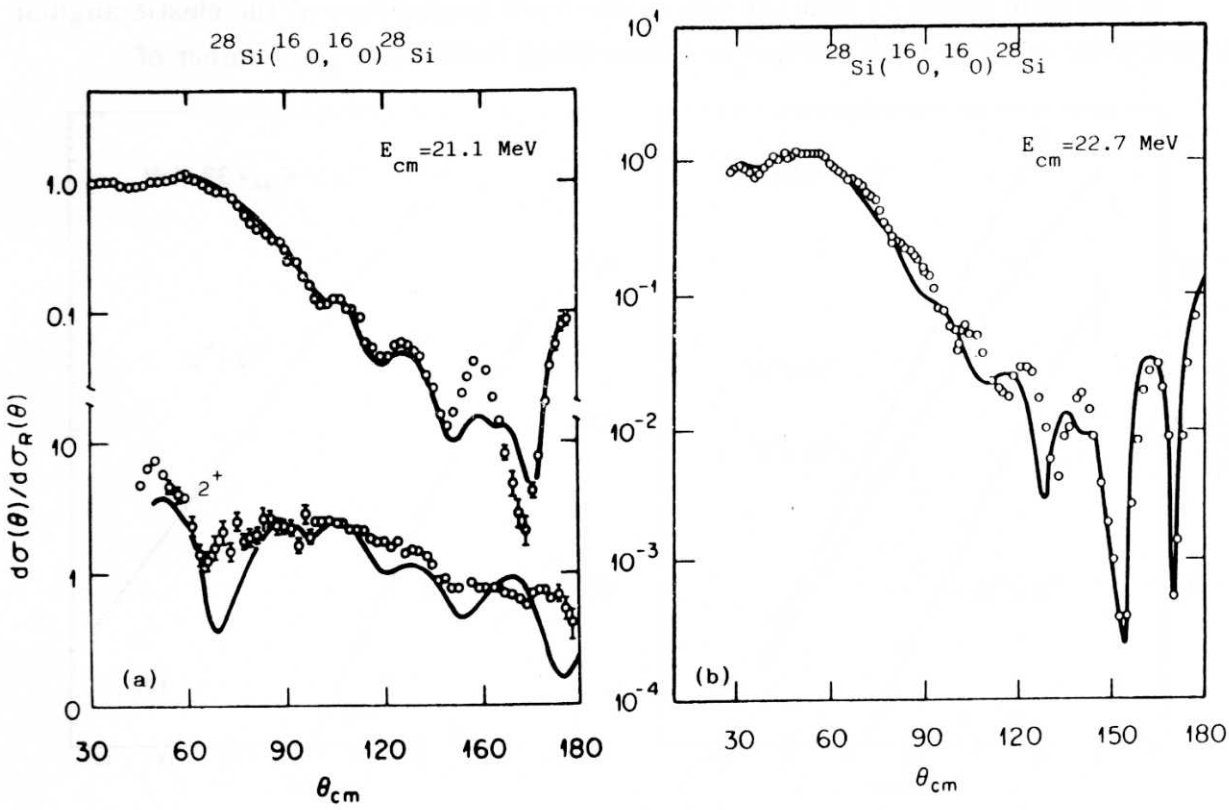

Fig. 4. *The ratio of elastic to Rutherford angular distributions for the reaction* $^{16}O + ^{28}Si$ *at two bombarding energies. In a) is also shown the differential cross section for the inelastic excitation of the* 2^+ *state in* ^{28}Si. *The curves correspond to coupled-channels calculations. The data points are from ref.* [15]).

In Fig. 4 are shown the calculated angular distributions in comparison with the experimental data for the bombarding energies $E_{c.m.} = 21.1\ MeV$ and $E_{c.m.} =$

22.7 MeV. For the lower bombarding energy the angular distribution for the excitation of the 2^+ state in ^{28}Si is also shown. In these calculations a very short-range volume-absorption with $W_0 = -2.5MeV$, $R = 5fm$ and $a = 0.2fm$ was added to the surface imaginary-potential of Table II. This is the only ingredient whose parameters have been adjusted to the data. From the short-range nature of this potential one may argue that its origin can be traced to massive transfers, for example α-transfer. A comparable fit to the experimental points could also be obtained[17]) using a shallower real potential and with a different volume absorption ($W_0 = -26.5MeV$, $R = 5.56fm$ and $a = 0.2fm$). In this last calculation the pronounced oscillations in the back hemisphere result from the coupling between the elastic channel and the rotational states in ^{28}Si. For both calculations it is essential to have a very weak absorption in the surface region so as to be sensitive to the real potential inside the Coulomb barrier (cf. also Ref. [18])).

3.3. *The* $^{16}O + ^{28,29,30}Si$ *excitation functions.*

It has been found[15]) that the rise in the back hemisphere of the elastic angular distribution of ^{16}O on Si isotopes is a decreasing function of the number of

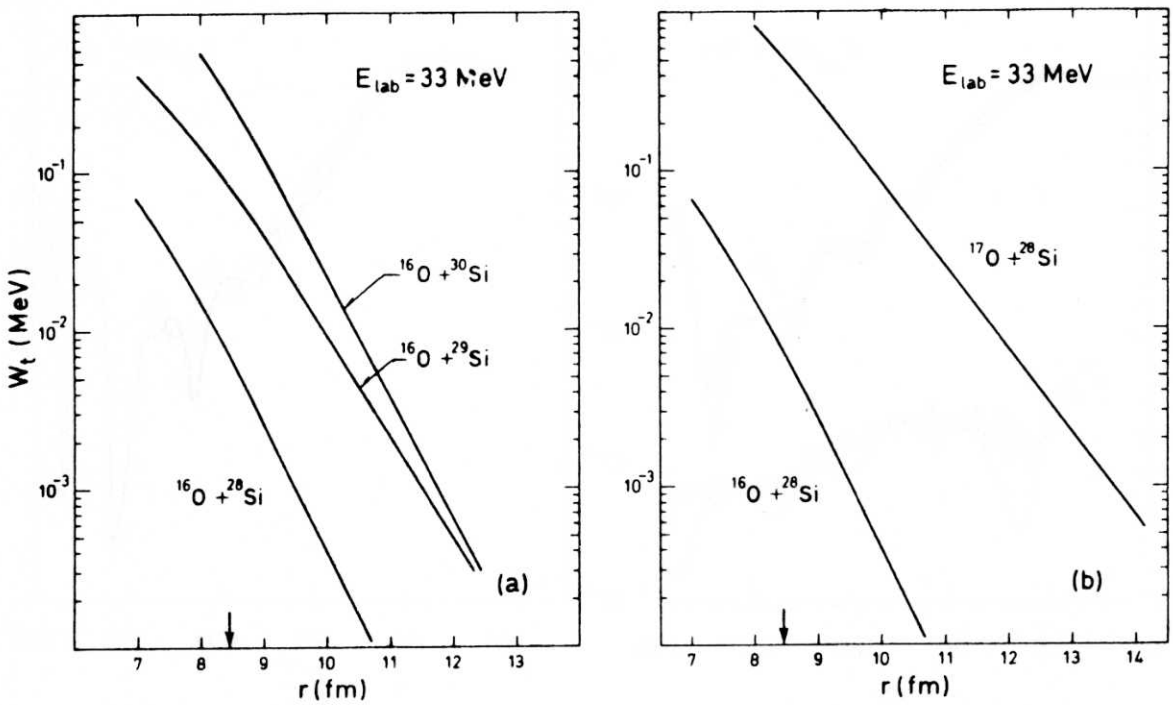

Fig. 5. *Absorptive potential arising from particle-transfer processes for the reactions (a) of* ^{16}O *on Si isotopes and (b) of O isotopes on* ^{28}Si *at the indicated bombarding energy.*

neutrons in the target. For example at $E_{c.m.} = 25MeV$ the cross section of ^{28}Si is 8% of Rutherford while it is only 2% in the case of ^{29}Si and only the 0.8% in the case of ^{30}Si. This finding suggests that the optical potential becomes less transparent as neutrons are added to the ^{28}Si core.

From the previous calculation we have learnt that the transparence of a potential is governed by the particle-transfer degrees of freedom. It is thus interesting to evaluate the imaginary potential W_{trans} for the three Si isotopes. Following the prescription outlined in the previous examples using the single-particle levels of Fig. 3 the imaginary potentials of Fig. 5a have been obtained[19]) at the bombarding energy $E_{lab} = 33MeV$. As can be seen, a substantial increase in the absorption is obtained by adding neutrons to the target thus explaining the decrease of the cross section at $\theta = 180^o$. Figure 5b displays the imaginary potential for the scattering of ^{17}O on ^{28}Si in comparison with the one of ^{16}O.

4. CONCLUSIONS

We have shown that the absorptive potential in heavy-ion reactions is dominated by the inelastic excitation and by the one-particle transfer reaction-channels. The first mechanism gives rise to an imaginary potential with a diffusivity $a = 0.3\ fm$ while the second one gives rise to a potential with a diffusivity $a = 0.6\ fm$. In applications we have shown how this interpretation of $W(r)$ can provide a way to extract selfconsistently, from the analysis of the data, nuclear-structure information like deformation parameters and spectroscopic factors. This model also gives insight in the use of transparent potentials for the study of the backward-rise phenomenon.

5. ACKNOWLEDGEMENTS

I would like to thank Prof. J. de Boer for carefully reading the manuscript of this paper and for helpful suggestions.

REFERENCES

[1] - R. A. Broglia, G. Pollarolo and A. Winther, Nucl. Phys. **A361** (1981)307.

[2] - G. Pollarolo, R. A. Broglia and A. Winther, Nucl. Phys. **A406** (1983)369.

[3] - R. A. Broglia and A. Winther, *Lecture notes on Heavy-Ion reactions, Vol. I* , Addison-Wesley, Reading, Mass., 1981.

[4] - T. Izumoto,S. Krewald and A. Faessler, Nucl. Phys. **A341**(1980)319; A. Faessler, T. Izumoto, S. Krewald and R. Sartor, Nucl. Phys. **A359** (1981)369.

[5] - R. Sartor and Fl. Stancu, Phys. Rev. **C26**(1982)1025;

[6] - N. Austern, *Direct Nuclear Reaction Theories,* J. Wiley, New York, 1970.

[7] - Bateman Manuscript Project, *Tables of Integral Transforms, Vol. II,*Mc Graw-Hill Book Company, New York 1954.

[8] - N. Anantaraman, Phys. Rev. **8C**(1973)2245.

[9] - F. Videbæk, thesis, Copenhagen.

[10] - O. Akyüz and A. Winther, in Proc. Enrico Fermi Inst. School of Physics, 1979, course on *Nuclear Structure and Heavy-Ion Reactions*. eds. R. A. Broglia, C. H. Dasso and R. Ricci (North Holland, Amsterdam, 1981)
[11] - F. G. Perey, GENOA code, unpublished.
[12] - C. H. Dasso, S. Landowne and G. Pollarolo, Nucl. Phys. 1985, in press.
[13] - J. M. Quesada, private comunication.
[14] - B. S. Nilsson, unpublished.
[15] - P. Braun-Munzinger and J. Barrette, Phys. Rep. **87**(1982) 209, and refs. therein.
[16] - G. Pollarolo and R. A. Broglia, Il Nuovo Cimento **81A** (1984)278
[17] - S. Kahana, G. Pollarolo, J. Barrette, R. A. Broglia and A. Winther, Phys. Lett. **113B**(1983)283.
[18] - A. M. Kobos and G. R. Satchler, Nucl. Phys. **A427**(1984)589.
[19] - J. M. Quesada, R. A. Broglia, V. Bragin and G. Pollarolo, Nucl. Phys. **A428**(1984)305c.